

# Comparison between different schemes for passivation of multicrystalline silicon solar cells by means of hydrogen plasma and front side oxidation

M. Ghannam, G. Palmers, H. E. Elgamel, J. Nijs, R. Mertens, R. Peruzzi,<sup>a)</sup>  
and D. Margadonna<sup>a)</sup>  
IMEC, Kapeldreef 75, 3001 Leuven, Belgium

(Received 5 October 1992; accepted for publication 15 December 1992)

Different schemes for passivation of solar cells fabricated using casted multicrystalline silicon from Eurosolare are investigated. The efficiency of solar cells with front side oxide surface passivation, front side and/or back side hydrogen plasma passivation are compared. It is shown that oxide passivation of the front surface combined with hydrogen passivation from the back side is the optimum passivation scheme. A 16.2% top efficiency is obtained on 4 cm<sup>2</sup> cells implementing this passivation scheme and a 16.8% top efficiency is estimated with an optimized ARC combination.

A significant increase in the efficiency of multicrystalline solar cells have been achieved by combining phosphorus gettering and rear aluminum treatments into the passivated emitter cell (PESC) process reaching an efficiency of 17.8% on 4 cm<sup>2</sup> cell fabricated on Osaka titanium wafers.<sup>1</sup> Phosphorus gettered Polix multicrystalline silicon has been used to realize a 15.6% efficient 4 cm<sup>2</sup> 180 μm thick solar cell<sup>2</sup> in which the emitter is oxide passivated and uniformly doped with phosphorus from a P<sub>2</sub>O<sub>5</sub> solid source. The emitter in this case was uniformly etched back after phosphorus predeposition to reach a sheet resistance of 55 Ω/□. It has been shown that the heavy P gettering (supergettering) performed on this material prior to the cell processing resulted in a significant improvement of the bulk quality and allowed the boron doped *p*<sup>+</sup>*p* back surface region to act as an effective back surface field (BSF). More recently, 15.8% efficient 4 cm<sup>2</sup> relatively thick (> 300 μm) solar cells have been realized on casted multicrystalline silicon from Eurosolare without BSF implementation.<sup>3</sup> Neither high temperature P gettering nor rear aluminum treatment were performed on this cell. On the other hand, the cell received at the very back end a low-temperature back side hydrogen plasma treatment.

In this work three different schemes of passivation are implemented on solar cells (4 cm<sup>2</sup>) fabricated on Eurosolare casted multicrystalline silicon material, and compared. Front side oxide passivation is the first passivation scheme with no additional treatments. In the second scheme a front side hydrogen plasma treatment is combined with a similar treatment from the back side. In this case the front side is not oxide passivated. Finally, the third passivation scheme combines the back side hydrogen plasma treatment with the front side oxide passivation. Note that combining oxide passivation and hydrogen plasma treatment on the front side has been avoided since it has been reported<sup>4</sup> that the hydrogen plasma attacks the passivating oxide layer and degrades its passivation properties.

Three groups of cells B1, B2, and DU representing the three passivation schemes are fabricated simultaneously

following a selective emitter process. The starting material is a 380 μm thick 1.6 Ω cm *p*-type as-cut Eurosolare casted multicrystalline silicon. The electron lifetime of this material is measured by means of a microwave contactless conductivity modulation technique and estimated to be around 5–6 μs. The process steps are summarized in Fig. 1. The saw damage is removed by etching the wafers in a strong acid solution consisting of a mixture of HF/HNO<sub>3</sub>/CH<sub>3</sub>COOH resulting in approximately 320–330 μm thick wafers with nicely polished surfaces. A masking CVD low-temperature oxide (Pyrox) layer 500 nm thick is deposited on the back side followed by a heavy P diffusion at 950 °C for 30 min from P<sub>2</sub>O<sub>5</sub> solid source wafers. This results in a 1 μm deep front side P diffused region with a sheet resistance of 8 Ω/□ (step 1). A CVD low-temperature oxide layer is then deposited on the front side and densified at 900 °C for 15 min in a wet oxygen ambient. The front side grid is patterned and the densified Pyrox is etched from the free area (front side active area). This is followed by a relatively deep etching of the silicon surface to totally remove the heavily P diffused layer from the active cell area. The heavily diffused region is protected from being etched under the front side grid pattern by the presence of the thick densified Pyrox layer. The latter is also used as a mask for selectively texturing the free active area. Random surface texturing of this area is carried out in a solution consisting of 2% NaOH-10% Isopropanol-88% H<sub>2</sub>O per weight at 80 °C for 30 min (step 2). The front side is completely cleared from the remaining Pyrox and a blanket solid source P diffusion is performed at 900 °C for 30 min resulting in a 0.75 μm deep 21 Ω/□ diffused layer in the active area and a 1.5 μm deep diffused layer under the front side grid pattern (step 3). The remaining protecting Pyrox at the back side is then removed. At this point of the process one group of cells (B2) is subjected individually to a front side hydrogen plasma treatment for 2 h (step 4). For this purpose, a rf (13.56 MHz) plasma reactor (PD80 from Plasma Technology) is used. The substrate to be passivated is put on the lower electrode with the side to be passivated facing the higher electrode. The treatment is carried out for 2 h maintaining the chuck temperature at

<sup>a)</sup>Eurosolare, Via d'Andrea 6, Nettuno 00048, Italy.

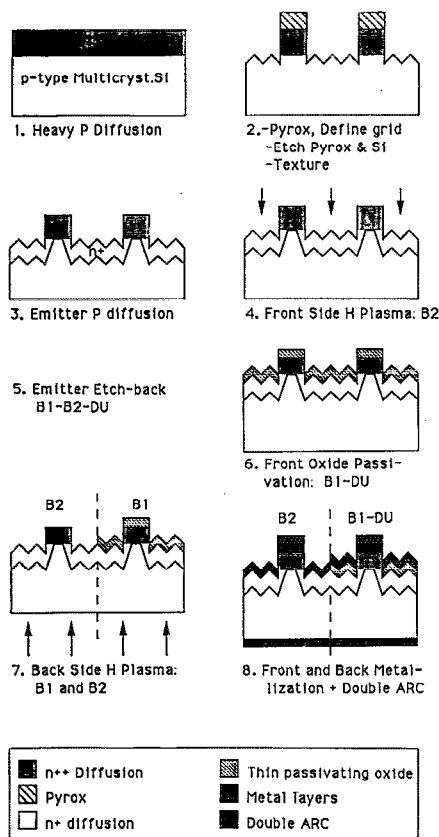


FIG. 1. Detailed processing steps for the three different groups: B1: front SiO<sub>2</sub> and back H, B2: front H and back H, DU: front SiO<sub>2</sub>.

350 °C, the plasma power density at 25 mW/cm<sup>2</sup> and the pressure at 600 mTorr. The heavily diffused surface dead layer is then removed for all groups by performing a blanket front side emitter etchback in a solution consisting of 1:100 per volume HF:HNO<sub>3</sub> for 17 s at room temperature resulting in an active emitter sheet resistance of 70 Ω/□ (step 5). Note that the front side hydrogen plasma treatment is performed prior to the emitter etchback rather than since it has been reported<sup>5</sup> this sequence results in a better performance due to the removal of the surface damage caused by the direct plasma. A thin passivating oxide layer (8 nm) is grown thermally at 900 °C for 6 min in a dry oxygen ambient on the surface of the wafers belonging to groups B1 and DU (step 6). A back side hydrogen plasma treatment at 350 °C for 3 h is applied to groups B1 and B2 (step 7). The front side metal contact grid is realized by *e*-beam evaporation of a triple metal layer Ti(50 nm)/Pd(50 nm)/Ag(5 μm) followed by liftoff and the

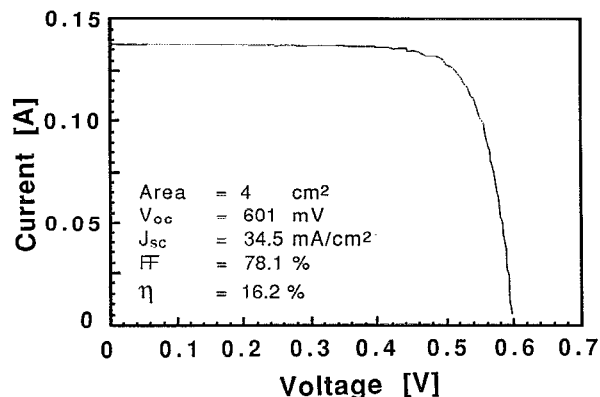


FIG. 2. *I-V* characteristics of the best cell belonging to group B1 under AM1.5 illumination conditions, at 25 °C.

back side metal contact is obtained by evaporation of a 2 μm layer of aluminum. This is followed by a sintering step at 400 °C for 20 min in forming gas. Such a relatively low sintering temperature is chosen in order to avoid the dissipation of the hydrogen atoms from the passivated cells. Cells with an area of 2×2 cm<sup>2</sup> are diced and the process is ended by the evaporation of a double antireflection coating consisting of 106 nm MgF<sub>2</sub> on top of 56 nm ZnS (step 8).

The parameters of the three groups of solar cells are listed in Table I. The cells of group B1 with front oxide and back hydrogen passivation show the best efficiency; the *I-V* characteristics under AM1.5 illumination of the best cell is displayed in Fig. 2. Back side hydrogen passivation leads to an increase in the efficiency of the front side oxide passivated cell from 15.3% (DU) to 16.2% (B1). As depicted in Fig. 3, the antireflection performance of group B1 is worse than that of group DU. With an identical antireflection performance for both groups, an additional 1% relative increase in the efficiency of the B1 cells is expected. Therefore, it is safe to say that the improvement in the efficiency due to hydrogen back side passivation amounts to 1% absolute.

On the other hand, the antireflection performance of the B2 cells is by far the best one, as Fig. 3 indicates. This behavior was expected since the double ARC system used here is optimized for minimum reflection from a bare silicon surface and not for a silicon surface with a thin oxide layer. When applying the optimum antireflection performance of group B2 to the B1 cells, a 3.5% relative increase in the short circuit current is estimated. This would raise the top value of the short circuit current of the B1 cells from 35 mA/cm<sup>2</sup> to at least 36 mA/cm<sup>2</sup> and the top effi-

TABLE I. Output performance of three types of solar cells (Global AM1.5 Spectrum of IMEC XT-10 Spectrolab sun simulator, 25 °C, cell area=4 cm<sup>2</sup>). A 4 cm<sup>2</sup> cell calibrated by NREL is used as a reference cell for the present efficiency measurements. Group B2 has an optimized ARC combination. Group B1 has the worst ARC performance.

Group	Front oxide	Front H	Back H	<i>J<sub>sc</sub></i> min	mA/cm <sup>2</sup> max	<i>V<sub>oc</sub></i> min	mV max	FF%		η%	
								min	max	min	max
B1	Yes	No	Yes	34	35.0	600	602	76.5	78.3	15.9	16.2
B2	No	Yes	Yes	32.8	33.8	592	594	77.5	79.3	15.3	15.6
DU	Yes	No	No	33	34.0	587	588	75.7	77.7	14.9	15.3

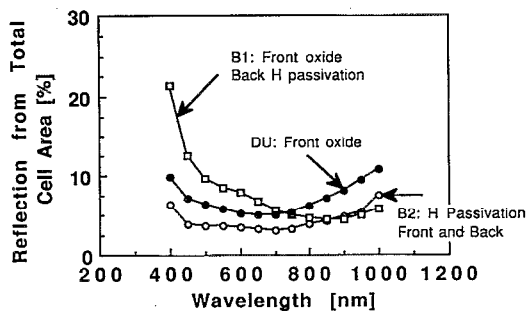


FIG. 3. Reflection measured on the total cell area ( $4 \text{ cm}^2$  with 4.5% metal) for the three type of cells.

ciency to 16.8%. These values seem to indicate that after back side hydrogen passivation the quality of the Eurosolare material becomes as good as that of the Osaka titanium large grain high quality multicrystalline silicon used in the reported 17.8% efficiency  $4 \text{ cm}^2$  cell<sup>1</sup> showing a similar value for  $J_{sc}$ . The higher open circuit voltage of the latter is due to the combined effects of a lower base resistivity, a back surface field effect created by the rear aluminum treatment and a highly perfected front surface oxidation technique resulting in a better quality front side oxide passivation.

The double sided-hydrogen passivated cells (B2) show a lower open circuit voltage and a lower short circuit current than the front side oxide passivated and back side hydrogenated cells (B1) despite the fact that the antireflection performance of group B2 is much better. This indicates that the front side hydrogen plasma passivation is not as efficient as front side oxide passivation, at least with the plasma conditions used here. A slight improvement in

$V_{oc}$  of the B2 cells is, however, observed compared to the front side oxide passivated and nonhydrogenated DU cells most probably due to the bulk passivation by hydrogen.

In summary, in this letter we demonstrate that the efficiency of  $4 \text{ cm}^2$  cells made on Eurosolare casted multicrystalline silicon can be improved by 1% absolute by back side hydrogen passivation. Clean oxidation is found to be the best technique for surface passivation. The results presented here indicate that combining back side hydrogen passivation and front side oxide passivation is the best scheme for improving the efficiency of multicrystalline silicon solar cells.

This work is supported by the Multichess Project of the JOULE program of the CEC, Project JOUR 0036. The authors are greatly indebted to P. De Schepper, W. Laureys, and P. Laermans from IMEC for their technical assistance throughout the processing of the cells as well as to F. Ferrazza from Eurosolare for the lifetime measurements.

<sup>1</sup>S. Narayanan, S. R. Wenham, and M. A. Green, *IEEE Trans. Electron Devices* **37**, 382 (1990).

<sup>2</sup>L. Q. Nam, M. Rodot, M. Ghannam, J. Coppye, P. de Schepper, J. Nijs, D. Sarti, I. Perichaud, and S. Martinuzzi, *Int. J. Solar Energy* **11**, 273 (1992).

<sup>3</sup>J. Nijs, M. Ghannam, J. Coppye, G. Palmers, L. Q. Nam, M. Rodot, S. Sivoththaman, and D. Sarti, paper 05.03 presented at the 11th European Community Photovoltaic Solar Energy Conference, Montreux, Switzerland, 12–16 October, 1992.

<sup>4</sup>J. Coppye, M. Ghannam, P. De Schepper, J. Nijs, and R. Mertens, *Proceedings of the 10th European Community Photovoltaic Solar Energy Conference, Lisbon, Portugal*, pp. 636–639 (1991).

<sup>5</sup>H. E. Elgamel, M. Y. Ghannam, J. Szlufcik, P. De Schepper, J. Nijs, R. Mertens, R. Peruzzi, and F. Ferrazza, paper 2A.05 presented at the 11th European Community Photovoltaic Solar Energy Conference, Montreux, Switzerland, 12–16 October, 1992.

*Published without author corrections*